ADVANCES IN FOREST FIRE RESEARCH

2022

Edited by

DOMINGOS XAVIER VIEGAS

LUÍS MÁRIO RIBEIRO

Analysis of thermal behaviour of merging fire fronts in crop field experiments

Alexander Filkov*; Brett Cirulis; Brendan Holyland; Trent Penman

University of Melbourne. VIC 3363 Australia,
{alexander.filkov, brett.cirulis, b.holyland, trent.penman}@unimelb.edu.au

**Corresponding author*

Keywords

Junction forward and backward fires, coalescence fires, parallel fire fronts

Abstract

Merging fires are known as destructive fires resulting in loss of life and houses. Despite growing efforts in the past decade to understand merging fires, there are still many knowledge gaps about their behaviour, especially at the field scale. In this study, we conducted experimental harvested crop burns in Victoria, Australia, in March and April 2021 to better understand thermal behaviour of merging fire fronts. UAVs with visual and thermal cameras were used to capture high-resolution fire propagation and the combustion process of merging fires. During experiments 50 junction fire fronts (32 forward and 18 backward) and 24 coalescence fire fronts were studied. For thermal analysis, 15 forward and 4 backward junction fire fronts, 6 coalescence fire fronts, and 10 parallel fire fronts were considered. Special methods were developed to process IR footages and compare the combustion process of merging fires and linear fire fronts (head and back fires). To do this, regions of interest (ROIs) containing the merging fire and linear fire front were selected in each frame using FLIR Research Studio. The ROIs were then exported using as bitmask images together with radiometric JPEG image containing both fires. Using the R programming platform, we determined the length and shape of the perimeter of fires for each JPEG image and defined buffer zones within the fire perimeter inside the ROI for each fire for further pixel temperature analysis. Thermal analysis showed that for forward junction fires the median temperature of head linear fire fronts was higher than forward junction fires except towards the end of merging. While in backward junction fires, the proportion of pixels with high temperature was much higher than in back linear fire fronts, indicating much larger burning areas. The temperature distributions of coalescence and parallel fires showed a decrease in the number of high-temperature pixels toward the end of the merge for coalescence and throughout for parallel fires. The fire behaviour observed in the field experiments demonstrates the necessity for better understanding of merging of fire fronts and the relationship between fuel, weather and fire line interaction.

1. Introduction

Over the past decade, extreme wildfires have occurred around the world with significant social, economic, and environmental consequences. They threaten the lives of many people and cause billions of dollars in damage. Climate change is further worsening fire seasons by increasing the number of dry and hot days (Bradstock 2010; Parente et al. 2018; Halofsky et al. 2020; Vilà-Vilardell et al. 2020). Longer fire seasons are expected to lead to more frequent and severe fires (Matthews et al. 2012; Di Virgilio et al. 2019). Such predictions were observed during the 2019/20 bushfire season in Australia (Filkov et al. 2020b).

These consequences are mainly the result of dynamic fire behaviours (DFBs) (Werth et al. 2011; Filkov et al. 2018; Tedim et al. 2018; Filkov et al. 2020a), which can lead to rapid increases in fire intensity and rate of spread (Hilton et al. 2017). Merging fires (Viegas 2012; Viegas et al. 2013; Thomas et al. 2017; Hilton et al. 2018; Raposo et al. 2018) is one of them. The convergence of separate individual fires into larger fires is called coalescence, and the merging of two lines of fire intersecting at an oblique angle is termed junction fire or junction fire fronts (Viegas 2012). Fire coalescence, junction and parallel fire fronts are all examples of merging fire fronts.

Most of experimental studies of merging fires have been conducted in the laboratory (Viegas et al. 2013; Oliveira et al. 2014; Sullivan et al. 2019), and only a few in the field (Raposo et al. 2018). Filkov et al. (2021) have demonstrated that the fire behaviour associated with merging fires in the field can be different and there remain ‘scale-gaps’ in the experimental data used to inform model development. Moreover, information about thermal behaviour of merging fires and burning depth is unknown. Therefore, the aim of this study was to develop materials that provide a better understanding of the dynamic nature of fire line merging.

1.1. Methods

Two experimental burns (Shelford and Lake Burrumbeet) on harvested wheat fields were conducted in Victoria, Australia, in March and April 2021. During experiments, junction fires, spot fire coalescence and parallel fire fronts were investigated.

Automatic Weather Station (AWS, 30 min temporal resolution) was used for air temperature and relative humidity measurements. Davis cup anemometer sensor in the Shelford burn (ICT International) and 2-dimentional DS-2 sonic sensors in the Lake Burrumbeet burn (Decagon Devices, Inc., Pullman, USA) with one min temporal resolution were used for wind direction and speed measurements. The terrain in both burns was relatively flat with minimal undulations. Fuel properties and weather condition are presented in Table 1.

Table 1- Fuel properties and weather characteristics

Burn name	Fuel height, cm	Fuel load, kg/m^2	MC, %	Wind speed, m/s	T, C	RH, %
Shelford	18.6±3.8	0.11±0.03	36±3	3.4±1.1.	27.4	44
Lake Burrumbeet	51.4±2.6	0.65±0.12	17±4.5	5.4±1.2	16	62

MC is the fine fuel moisture content (wet basis), T is the air temperature at 15:00, RH is the relative humidity at 15:00, ± is the standard deviation

Two UAVs, a DJI Mavic Pro (Shelford burn) and DJI Matrice 210 (Lake Burrumbeet burn) were used to capture high-definition video imagery of fire propagation. DJI Mavic Pro is equipped with visual camera (3840×2160 pixels, 30 Hz). The camera model used with the DJI Matrice 210 was the XT2 payload with dual visual (3840×2160 pixels, 30 Hz) and thermal (640x512 pixels, 30 Hz) video capability. XT2 payload allows to film simultaneously both visual and thermal (radiometric) videos. The post processing phase was completed for each separate visual and thermal video and metadata file using the Full Motion Video (FMV) toolbox within the ArcGIS Pro 2.8.0 software (Macdonald 2017). The result is a video file with each frame georeferenced. The multiplexed video file was then used to identify and spatially define fire fronts at set time intervals.

After starting the ignition line, the fire front produced fire tongues. When the fire lines of two neighbouring tongues naturally merged together, we identified it as junction fire fronts (forward junction fire fronts) and the angle between them as an initial angle. If the junction fire fronts were spreading opposite to the direction of the head linear fire front, we identified them as the backward junction fire fronts. Two spot fires spreading toward each other were identified as coalescence fires. Two fire fronts burning parallel to each other and propagating towards each other were identified as inward parallel fire fronts. We measured travelling distance of the merging fire fronts every 2-5 seconds to calculate ROS. To estimate the effect of merging fire fronts on fire propagation we compared them with head and back linear fire fronts. The ROS of the linear fire front was measured in the vicinity to each merging fire front for their entire duration.

To analyse the effect of merging fire fronts on fire behaviour and thermal energy release, we compared the temperatures above 200 °C on thermal images of merging fires and linear fire fronts. Since the junction and linear fire fronts are very different in length and shape of the fire perimeter, we required a method for their relative comparison. To do this, we compared the temperature of pixels inside the buffer zones for each fire. In order to define them, we had to delineate linear and junction fires and determine their perimeters on thermal images. This process is different for each type of merging fires. For junction fires, we first manually created two regions of interest (ROIs) containing a junction fire and a section of a linear fire front on the thermal video (head and back linear fire fronts for forward and backwards junction fire fronts, respectively) using FLIR Research Studio 2.0.0. For parallel fire fronts and coalescence fires, we created one ROI containing both parallel fire fronts (their sections) and coalescence fires (complete fires).

The ROIs were then exported using FLIR Research Studio 2.0.0 as bitmask images together with radiometric JPEG image containing both fires. All images were exported at 2-, 4- or 5-second intervals, starting from the formation of the merging fire to its transition to a linear fire front for junction fires (180-degree junction angle) or to the moment of joining parallel or coalescence fires. Using the R programming platform 4.1.0 (R Core

Team 2021), we determined the length and shape of the perimeter of the merging and linear fires for each JPEG image. Using this information and the st_buffer function in R (sf package), we defined buffer zones within the fire perimeter inside the ROI for each fire for further analysis. We then analysed the temperatures of pixels, after which we calculated the temperature distributions for each time step. Due to different time duration of each merging fire, we converted time steps to percentages of final time.

2. Results and discussion

The use of a drone with a dual visual and thermal camera showed that the thermal camera was able to detect all active hot spots and fire fronts even through dense smoke, which was a significant constraint in our previous study (Filkov et al. 2021).

Thirty-four videos were filmed and multiplexed. Seventy-four merging fire fronts (42 in Shelford and 32 in Lake Burrumbeet burn) were identified: 50 junction fire fronts (32 forward and 18 backward) and 24 coalescence fire fronts. For thermal analysis, 15 forward and 4 backward junction fire fronts, 6 coalescence fire fronts, and 10 parallel fire fronts were considered since the amount of available thermal video footage was limited.

The combined ROS of forward, backward and head linear fire fronts had the highest median ROS for forward junction fires (2.02 m/s), followed by head linear and backward ROS, 0.67 m/s and 0.18 m/s, respectively. The ROS of the head linear fire fronts changed mostly in the range 0.1-2 m/s during the lifetime of the merging fires. A comparison of the median ROS values for forward junction fires and head linear fire fronts between the two burns showed that the difference was very consistent. Forward junction fires were 3 times faster than head linear fire fronts, 3.02 and 3.11 times faster for the Shelford and Lake Burrumbeet burns, respectively. The ROS of backward fire fronts is consistent between the two burns, 0.17-0.2 m/s. Although the average ROS of forward junction fires was 3 times that of head linear fire fronts, it was up to 18 times higher than head linear fire fronts in some cases.

The pixel temperature distribution within the buffer zones for merging fires is presented on Fig. 1. Data analysis for forward junction fires showed that the median temperature of head linear fire fronts was higher than forward junction fires except towards the end of merging (Fig. 1a). In backward junction fires, the proportion of pixels with high temperature was much higher than in back linear fire fronts (Fig. 1b). For example, the difference in median temperature between the two ranged from 100 to 200 °C, indicating much larger burning areas in the backward junction fires. Non overlapping notches in all groups indicate with a 95% confidence level that the temperature medians for junction fires and linear fire fronts are different.

Analysis of temperatures above 500 ºC in forward junction fires, representing flaming combustion in wildfires (Wotton et al. 2011), showed that the density of high-temperature pixels (above 500 °C) increases, and the temperature peak shifts toward higher temperatures during the merging process. Whereas for head linear fire fronts, the temperature density and its peak remain practically unchanged. It was expected that the density of "hot" pixels should be higher for forward junction fires compared to head linear fire fronts during the merging process. Higher ROS should have resulted in more fuel burning simultaneously and larger "deep flaming" areas. However, we found that only in the last stage of merging (75% and 100% time) was the median temperature and temperature range higher and larger. It is assumed that the “deep flaming” is a consequence of the forward junction fires and not a mechanism of their propagation. Liu et al. (2021) in their literature review discuss potential mechanisms of fire merging and point to interacting air entrainment fields and enhanced heat feedback to fuels. In our study, we did not have the opportunity to study convection, but it will be addressed in future studies.

Unexpected results were also received for coalescence fires (Fig. 1c). Although, the ROS increases over time, its value decreases as the distance between two spot fires decreases. At this point, we have no explanation for these results. The temperature distribution also showed a decrease in the number of high-temperature pixels toward the end of coalescence. One possible explanation for this is that in our analysis we assumed that the end of coalescence is the time when the two fires joined together, but not the time when they completely merged to form one fire. Additional experiments and analysis are needed to explain the above results.

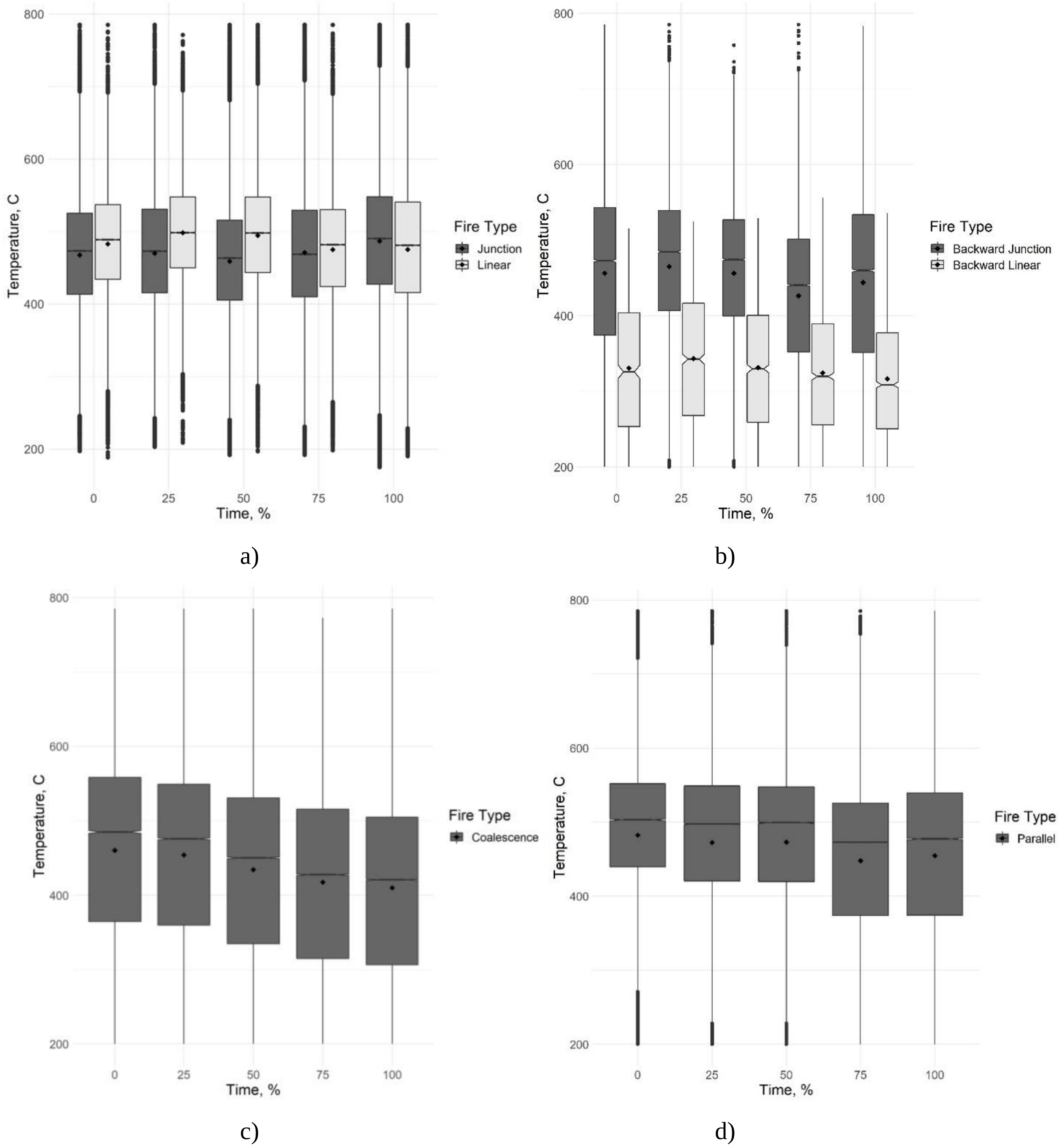

Figure 1- A notched box plot of the distribution of pixel temperature in the buffer zone of the merging fires: a) the forward junction fire (Junction) and head linear fire front (Linear) for the duration of forward junction fire; b) the backward junction fire (Backward junction) and back linear fire front (Back linear) for the duration of backward junction fire; c) the coalescence fires; d) the parallel fires. Time is dimensionless. Zero percent is the moment of formation of the merging fire, 100% is the moment of transition to the linear fire front (180-degree junction angle) or to the moment of joining parallel or coalescence fires. Boxes contain 50% of data. Dots represent outliers. Line is the median and rhombus is the mean.

Parallel fire, opposite to forward junction fires, had a decrease in the number of high-temperature pixels by the end of merging.

Our study has a few limitations. The drone thermal camera is factory calibrated to 550 °C. Values above this value are extrapolations in the FLIR software. They should be analysed with caution. In our future study we are going to use a thermal filter to extend the temperature range. Also, comparing thermal pixels within buffer zones of merging fires and linear fire fronts may not be the best option.

3. Conclusion

Conducted field experiments have confirmed that merging fires behave differently than regular fires (linear fire fronts), and standard operational models will underestimate fire behaviour when merging occurs. In some cases, the forward ROS of forward junction fires can be up to 18 times higher than the head linear ROS. Analysis of the thermal footages revealed that a greater number of pixels with higher temperatures were observed at the end of fires merging in forward junction fires and during the entire merging time in backward junction fires compared to linear fire fronts. These results indicate the danger that junction fires can pose to firefighters and communities and the need to incorporate them into fire behaviour models. Further research is needed to better understand the unexpected temperature behaviour of coalescence and parallel fires.

4. References

Bradstock, RA (2010) A biogeographic model of fire regimes in Australia: current and future implications. Global Ecology and Biogeography 19, 145-158.

Di Virgilio, G, Evans, JP, Blake, SAP, Armstrong, M, Dowdy, AJ, Sharples, J, McRae, R (2019) Climate Change Increases the Potential for Extreme Wildfires. Geophysical Research Letters 46, 8517-8526.

Filkov, A, Cirulis, B, Penman, T (2021) Quantifying merging fire behaviour phenomena using unmanned aerial vehicle technology. International Journal of Wildland Fire 30, 197-214.

Filkov, AI, Duff, TJ, Penman, TD (2018) Improving fire behaviour data obtained from wildfires. Forests 9, 1-21.

Filkov, AI, Duff, TJ, Penman, TD (2020a) Frequency of Dynamic Fire Behaviours in Australian Forest Environments. Fire 3, 1-19.

Filkov, AI, Ngo, T, Matthews, S, Telfer, S, Penman, TD (2020b) Impact of Australia's catastrophic 2019/20 bushfire season on communities and environment. Retrospective analysis and current trends. Journal of Safety Science and Resilience 1, 44-56.

Halofsky, JE, Peterson, DL, Harvey, BJ (2020) Changing wildfire, changing forests: the effects of climate change on fire regimes and vegetation in the Pacific Northwest, USA. Fire Ecology 16,

Hilton, J, Sharples, J, Sullivan, A, Swedosh, W, 2017. Simulation of spot fire coalescence with dynamic feedback. 22nd International Congress on Modelling and Simulation, Hobart, Tasmania, Australia, 3 to 8 December 2017. 1111-1117.

Hilton, JE, Sullivan, AL, Swedosh, W, Sharples, J, Thomas, C (2018) Incorporating convective feedback in wildfire simulations using pyrogenic potential. Environmental Modelling and Software 107, 12-24.

Liu, N, Lei, J, Gao, W, Chen, H, Xie, X (2021) Combustion dynamics of large-scale wildfires. Proceedings of the Combustion Institute 38, 157-198.

Macdonald, O (2017) Getting to know ArcGIS Pro. Cartographic Journal 54, 284-285.

Matthews, S, Sullivan, AL, Watson, P, Williams, RJ (2012) Climate change, fuel and fire behaviour in a eucalypt forest. Global Change Biology 18, 3212-3223.

Oliveira, LA, Lopes, AG, Baliga, BR, Almeida, M, Viegas, DX (2014) Numerical prediction of size, mass, temperature and trajectory of cylindrical wind-driven firebrands. International Journal of Wildland Fire 23, 698-708.

Parente, J, Pereira, MG, Amraoui, M, Fischer, EM (2018) Heat waves in Portugal: Current regime, changes in future climate and impacts on extreme wildfires. Science of the Total Environment 631-632, 534-549.

R Core Team (2021) 'R: A language and environment for statistical computing. R Foundation for Statistical Computing.' Vienna, Austria)

Raposo, JR, Viegas, DX, Xie, X, Almeida, M, Figueiredo, AR, Porto, L, Sharples, J (2018) Analysis of the physical processes associated with junction fires at laboratory and field scales. International Journal of Wildland Fire 27, 52-68.

Sullivan, AL, Swedosh, W, Hurley, RJ, Sharples, JJ, Hilton, JE (2019) Investigation of the effects of interactions of intersecting oblique fire lines with and without wind in a combustion wind tunnel. International Journal of Wildland Fire 28, 704-719.

Tedim, F, Leone, V, Amraoui, M, Bouillon, C, Coughlan, RM, Delogu, MG, Fernandes, MP, Ferreira, C, McCaffrey, S, McGee, KT, Parente, J, Paton, D, Pereira, GM, Ribeiro, ML, Viegas, DX, Xanthopoulos, G (2018) Defining Extreme Wildfire Events: Difficulties, Challenges, and Impacts. Fire 1, 1-28.

Thomas, CM, Sharples, JJ, Evans, JP (2017) Modelling the dynamic behaviour of junction fires with a coupled atmosphere-fire model. International Journal of Wildland Fire 26, 331-344.

Viegas, DX, 2012. Extreme Fire Behaviour. Forest Management: Technology, Practices and Impact. Nova Science Publishers, Inc., 1-56.

Viegas, DX, Raposo, J, Figueiredo, A (2013) Preliminary analysis of slope and fuel bed effect on jump behavior in forest fires. Procedia Engineering 62, 1032-1039.

Vilà-Vilardell, L, Keeton, WS, Thom, D, Gyeltshen, C, Tshering, K, Gratzer, G (2020) Climate change effects on wildfire hazards in the wildland-urban-interface – Blue pine forests of Bhutan. Forest Ecology and Management 461, 117927.

Werth, PA, Potter, BE, Clements, CB, Finney, MA, Goodrick, SL, Alexander, ME, Cruz, MG, Forthofer, JA, McAllister, SS (2011) Synthesis of knowledge of extreme fire behavior: Volume I for fire management. US Department of Agriculture, Forest Service, Pacific Northwest Research Station No. Gen. Tech. Rep. PNW-GTR-854, Portland, OR.

Wotton, BM, Gould, JS, McCaw, WL, Cheney, NP, Taylor, SW, Wotton, BM, Gould, JS, McCaw, WL, Cheney, NP, Taylor, SW (2011) Flame temperature and residence time of fires in dry eucalypt forest. International Journal of Wildland Fire 21, 270-281.